CHAPTER 2

SYNTHESIS AND CHARECTERIZATION OF Mn(II), Fe(II), Co(II), Cu(II), Zn(II) COMPLEXES OF 3,5-DI NITRO BENZOIC ACID, CRYSTAL STRUCTURES OF Co(II) AND Cu(II)

2.1 Introduction

The Mn, Fe, Co, Cu and Zn all are belonged in 1st transition metal series because the last electron in the atoms of these elements enters in d-sub-shell belonging to penultimate shell. Most of the transition metals show more than one oxidation states. Because of the presence of 'd' electron these transition metals display different oxidation states and sometimes form complexes with the same ligand in different oxidation state. This is generally true for the complex compounds of transition metal chemistry and is a subject of interest for years due to not only of its rich structural chemistry but also for its versatile applications. It is now well recognized that in the human body minute amount of many elements can be detected and estimated. Some of these elements have been shown to be essential for life. They are involved in all major metabolic pathways of life. They serve a variety of functions that include catalytic, structural and regulatory activities in which they interact with various enzymes and biological membranes [1]. Iron functions as a cofactor for enzymes involved in many metabolic processes, including oxygen transport, DNA synthesis, electron transport and are transformed into biologically available form in the mitochondrion by the iron-sulphur cluster and haeme synthesis pathway [2]. Zinc plays an important roles in nucleic acid metabolism, cell replication, tissue repair and growth, as well as zinc-containing nucleoproteins are involved in gene expression of multiple proteins [3,4]. The Cu is present in the oxygen carrying system in blood of many invertebrates and is a major constituent of many enzymes and proteins [5]. The Mn is an essential element to be found in all tissues. It is needed for metabolism of amino acids, lipids, proteins and carbohydrates as well as it takes part in the defense of red blood cells in the metabolism of iron [6]. It is well known that Co is an essential metal necessary for the formation of vitamin B_{12} [7]. The important role of Mg in chlorophyll is well established in green plant system. But all the metals are essential in small amounts; in large amounts, however, these may endanger the life processes. Small amounts of Fe, Cu, Zn etc. are found as growth and development agents of fungi. Whereas, e.g, Cu and Zn when incorporated in some organic ligands act as important fungicide. The (more toxic metals) Hg and Pb compounds can also

act as fungicides [8]. Further many transition metal complexes are associated with biological and commercial applications [9-15].

2.2 Literature

Several cupric carboxylates are dimeric either in the crystalline state, in solution or in both [16]. Considerable controversy has been caused over the mode of bonding in the dimeric Cu(II) acetate monohydrate [17]. The main cause of the problem possibly arises from the method of preparation of the complexes. Frequently, they are isolated as hydrates or solvates followed by dehydration under vacuum. The application of heat to these complexes may cause slight decarboxylation of the compounds affording anhydrous materials contaminated with small amounts of copper oxide in insufficient quantities to affect the elemental analysis [18]. This contamination of the complex would significantly affect the magnetic properties. So the bonding mode of dimeric Cu(II) acetate is debatable [17]. Kumar and Suri [19] have reported that the adducts of copper (II) aryl carboxylates with morpholine can be prepared by interacting the reactants in 1:1 molar ratio or using a large excess of morpholin in acetone medium. Analytical results show that the adducts are either mono-morpholine or bis-morpholine of 1:1 or 1:2 stoichiometry formulated as $Cu(O_2CC_6H_4R)_2(morph)_n$ where R is H, CH_3-o, CH_3-m, Cl-o, Cl-m, Br-o, Ch_3O-o, Ch_3O-m, Ch_3O-p, NO_2-o, NO_2-m, NO_2-p, OH-o, OH-m, and $OCOCH_3$-o; Morph is Morpholine and n is 1 or 2. Conductance measurements show that all these adduct are non-ionic. Magnetic and electronic spectral studies suggest that mono-morpholin adducts are dinuclear syn-syn carboxylate bridge species whilst bis-morpholin adducts are mononuclear distorted octahedral molecules. IR-spectra show that morpholin behaves as a N-bonded monodentate ligand [19-20]. J. Bickley and his coworkers [21] have described the synthesis and crystal structures of two new copper complexes with chelating dicarboxylic acids. Reaction of copper(II) acetate with diacid H_2**L2** ($HO_2CC(Me)_2OArOC(Me)_2CO_2H$, Ar=1,3-substituted phenyl) gave a bischelate complex (**L2**)$_2Cu_2 \cdot 2MeOH$ (Fig. 2.1) with the normal paddlewheel structure and tilted, *trans*-oriented chelate rings with skewed conformations. The overall structure was reasonably well reproduced by density functional calculations on (**L2**)$_2Cu_2$. Treatment of the product from reaction of $Cu_2(OAc)_4$ and diacid H_2**L3** (Ar=1,3-substituted 2,4-dibromophenyl) with pyridine gave a six-coordinate

mononuclear chelate (**L3**)$Py_2Cu \cdot H_2O$ (Fig. 2.2) in which one chelate carboxylate is monodentate, the other is unsymmetrically bidentate and the pyridines are *cis*-coordinated.

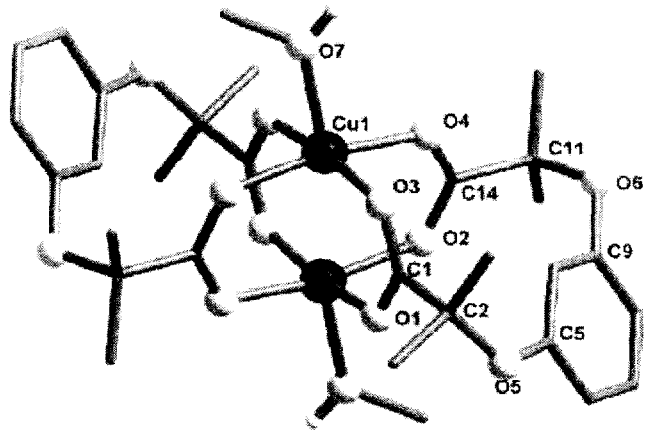

Fig. 2.1 Structure of $(L2)_2Cu_2 \cdot 2MeOH$ [21].

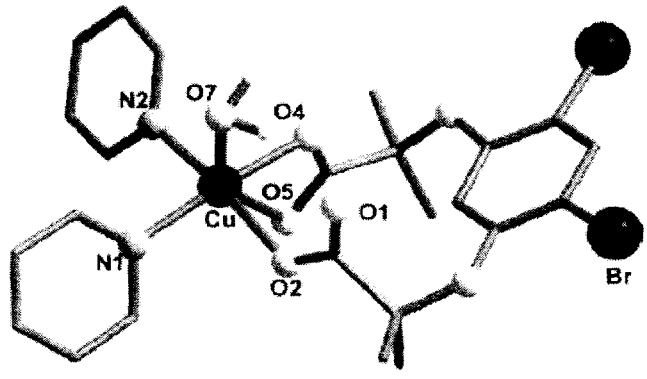

Fig. 2.2 Structure of $(L3)Py_2Cu \cdot H_2O$ [21].

In 1998, the dinucleating ligand *N,N'*-(2-hydroxy-5-methyl-1,3-xylylene)bis(*N*-(carboxymethyl)glycine) (CH_3HXTA) has been used to synthesize the dinuclear Cu(II) bis(pyridine) complex $Na[Cu_2(CH_3HXTA)(Py)_2] \cdot 1.5$(1,4-dioxane) [Na(**1**)]: triclinic. The structure shows two distinct distorted square pyramidal Cu(II) centers with each Cu(II) ion bound by two carboxylate oxygen atoms, one amine nitrogen atom, a phenolate oxygen atom, and one pyridine nitrogen atom. The phenyl ring of the CH_3HXTA ligand is twisted relative to the Cu1-O1-Cu2 plane, and the resulting dihedral angle is 44.2°. The electronic absorption spectrum of **1** in aqueous solution at pH 3 suggests a shift toward trigonal bipyramidal Cu(II) coordination in

solution. Spectral titration of $Na[Cu_2(CH_3HXTA)(H_2O)_2]$ (Fig. 2.3) with L (where L= pyridine or sodium cyanide) results in complexes with terminal L groups. These exogenous ligands appear to bind in a positive cooperative stepwise fashion. Variable-temperature magnetic susceptibility data for **1** indicate that the Cu(II) ions are antiferromagnetically coupled ($-2J = 168\ cm^{-1}$). The ^1H NMR studies on a methanol solution of **1** are consistent with weak spin-coupling in solution [22].

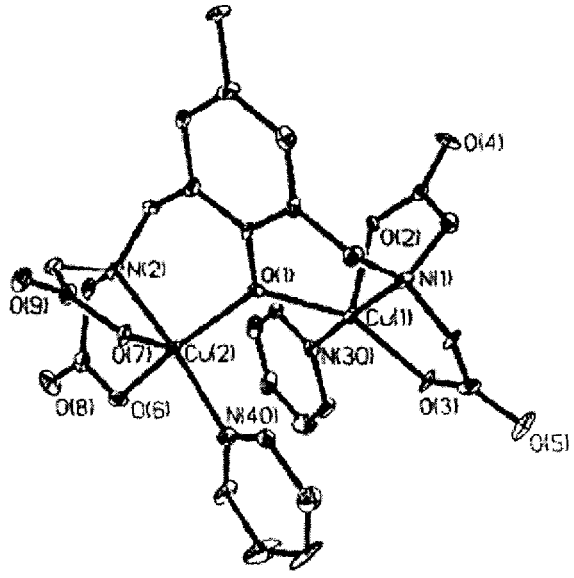

Fig. 2.3 Structure of $[Cu_2(CH_3HXTA)(Py)_2]^-$ anion [22].

Akopova *et al.* [23] described the synthesis, structure, and mesomorphism of a new series of copper carboxylates **Ia-f** (Fig. 2.4). Compounds **Ia,b,c,e** were obtained by fusing copper hydroxide with the corresponding acid, while compounds **Id,f** were obtained by the exchange reaction.The influence of periphery of the chelate node on the appearance of discophase was studied. A stacked hexagonal structure of copper erucate was proved. The effect of restructuring of the chelate node in this compound after its isothermic exposure, causing the loss of mesomorphism was revealed.

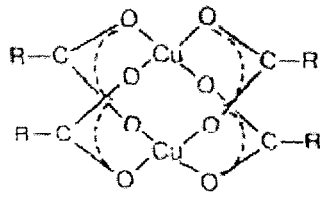

1a–f

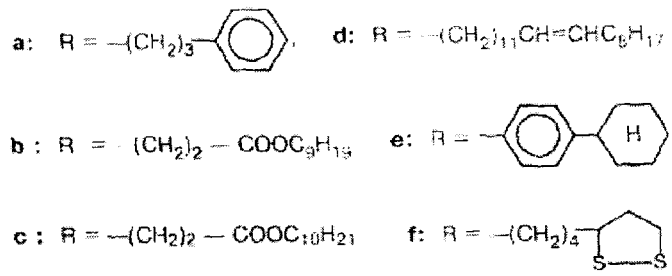

Fig. 2.4 Structure of copper carboxylate [23].

Kozlevčar *et al.* [24] during the investigations of fatty acid copper(II) carboxylates with biologically important ligands prepared several compounds of the composition $[Cu_2(O_2CC_nH_{2n+1})_4(urea)_2]$ (n = 5 to 11) and $[Cu_2(O_2CC_5H_{11})_4(urea)_2]$. The molecular structure of the compound $[Cu_2(O_2CC_5H_{11})_4(urea)_2]$ (Fig. 2.5) was determined by X-ray diffraction analysis. The compounds were characterized by standard physical and chemical methods and tested for their fungal mycelial growth inhibition activity with mycelia of two wood decay fungi *Trametes versicolor* and *Antrodia vaillantii*. The results of the characterization are in agreement with the values typical for dimeric copper(II) carboxylates. In the electronic spectra the difference between both types of hexanoate compounds was observed, however in vibrational spectra also the differences among the compounds where one molecule of urea is bonded on each dimmer were noticed. Significantly higher growth inhibition for the whole series for *Antrodia vaillantii* was observed.

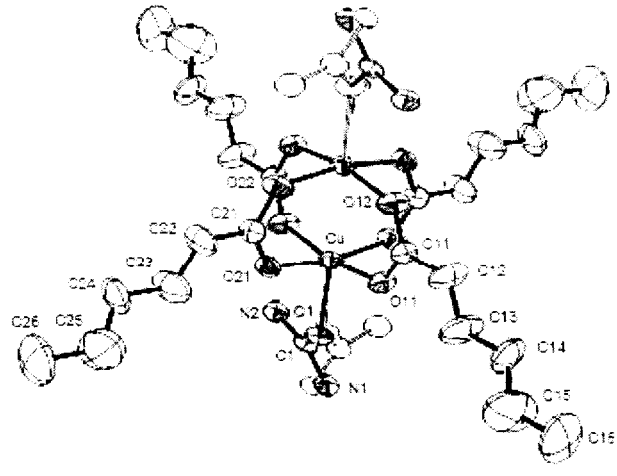

Fig. 2.5 Structure of $[Cu_2(O_2CC_5H_{11})_4(OCN_2H_4)_2]$ [24].

Waizump *et al.* [25] have reported the synthesis and crystal structures of $[Co(nic)_2(H_2O)_4]$ (**1**). $[Co(iso)_2(H_2O)_4]$ (**2**). $[Cu(nic)_2(H_2O)_4]$ (**3**), and $[Cu(iso)_2(H_2O)_4]$ (**4**) (nic = nicotinate; iso = isonicotinate) (Fig. 2.6). The crystal of complex **1** is monoclinic, space group *C2/m* and the other crystals **2** **3** and **4** are all triclinic. The arrangements around the metal ions are *trans*-octahedra with two pyridyl nitrogen and two aqua oxygen in the equatorial positions and two aqua oxygen in the axial positions, although the Cu(II) complexes show a larger Jahn-Teller distortion.

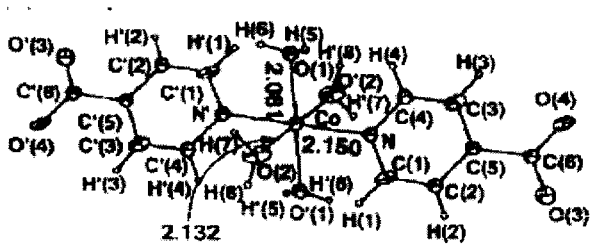

Complex **2**

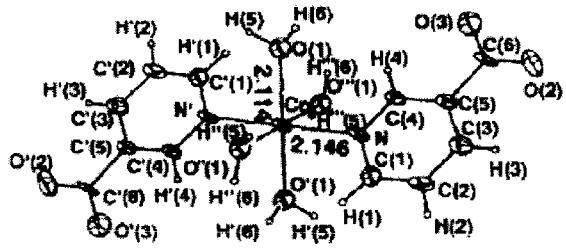

Complex **1**

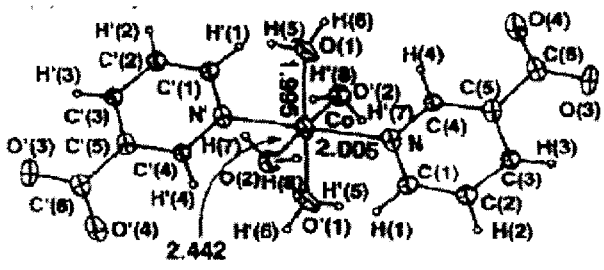

Complex **3**

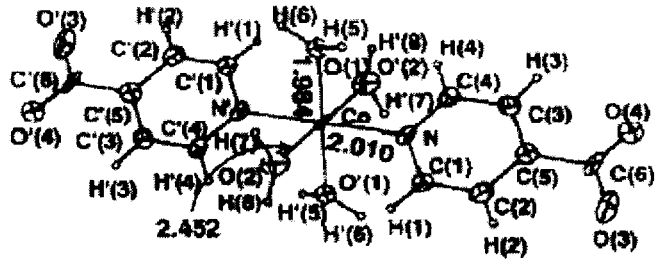

Complex **4**

Fig. 2.6 Crystal structures of $[Co(nic)_2(H_2O)_4]$ (**1**). $[Co(iso)_2(H_2O)_4]$ (**2**). $[Cu(nic)_2(H_2O)_4]$ (**3**) and $[Cu(iso)_2(H_2O)_4]$ (**4**) (nic = nicotinate; iso = isonicotinate) [25].

Very recently, a Chinese group has synthesized a new complex, $Co(MBTC)_2(DMF)_2$ (MBTC□6-methoxybenzothiazole-2-carboxylate, DMF□*N*,*N*-dime- thylformamide), in DMF solution and characterized by single crystal X-ray diffraction analysis. Using the cobalt complex as catalyst, phenylacetic acid was prepared by the carbonylation of benzyl chloride with carbon monoxide (0.1 MPa). The effects of solvents, phase transfer catalysts and temperature on the reactions were investigated. The yield of phenylacetic acid was higher than 90% in optimized conditions [26]. Vučković *et al.* [27] reported novel binuclear Co(II) complexes with *N*-functionalized cyclam, *N*,*N*',*N*'',*N*'''-tetrakis (2-pyridylmethyl) tetraazacyclotetradecane (tpmc) and one of the aromatic mono or dicarboxylato ligands (benzoate, phthalate or isophthalate ions). The compounds were analyzed and studied by elemental analyses (C, H, N), electrical conductivities, VIS and IR spectroscopy and magnetic as well as cyclic voltammetric measurements. In $[Co_2(C_6H_5COO)_2tpmc](ClO_4)_2 \cdot 3H_2O$ (Fig. 2.7), the benzoate ligands are most probably coordinated as chelates in the *trans*-position to each Co(II) and the macrocycle adopts a *chair* conformation. In the complexes $[Co_2(Y)tpmc](ClO_4)_2 \cdot zH_2O$, (Y = phthalate or *i*-phthalate dianizon, z = 2; 4), it is proposed that the isomeric dicarboxylates are bonded combined as bridges and chelates. The composition and the assumed geometries of the complexes are compared with the, earlier reported, corresponding Cu(II) complexes. Cyclic voltammetry measurements showed that the compounds are electrochemically stable.

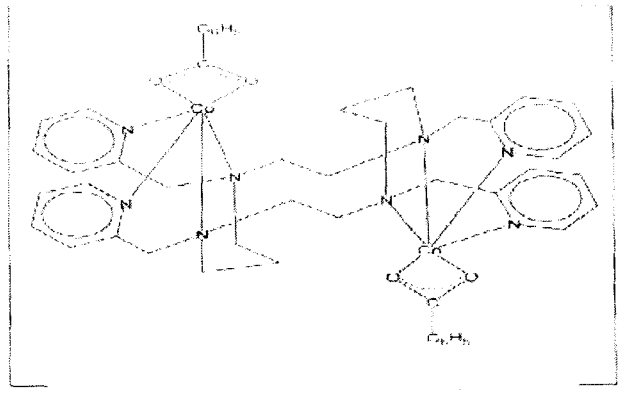

Fig. 2.7 Suggested structure of the $[Co_2(C_6H_5COO)_2tpmc]^{2+}$ from complex (**1**) in a *chair* conformation [27].

T. A. Zevaco and his coworkers [28] in 1998, have published a paper covering the synthesis, spectral characterization and X-ray structure determination of the zinc(II) norbornen-2,3 dicarboxylate [Zn(*cis*-2,3-ndc)-(1-methylimidazole)$_2$(H_2O)]$_\infty$ (**1**) (*cis*-2,3-ndc = bicyclo[2,2,1]-hept-5-ene-2,3-*cis*-dicarboxylic acid). It crystallizes in the monoclinic space group $P2_1/c$. The crystal structure of **1** consists of polymeric chains which propagate along the *c* axis. The structure is stabilized by extended hydrogen bonds involving adjacent chains and water molecules. The metal centers display a slightly distorted tetrahedral geometry. The norbornenedicarboxylic acid acts as a *syn*-bound O,O′-bridging ligand. In the same year they also published another paper which was covering the reaction of an aqueous suspension of zinc oxide with 2-quinolinecarboxylic acid afforded, after recrystallization from a 1-methylimidazole/ acetonitrile solution, crystals of the anhydrous carboxylate [Zn(2-quinolinecarboxylato)$_2$ (1-methylimidazole)$_2$]. **1** [Zn($C_{10}H_6NO_2$)$_2$ ($C_4H_6N_2$)$_2$], monoclinic, space group $P2_1/n$. The zinc atom is hexacoordinated, located at an inversion center and exhibits a slightly distorted ctahedral geometry. The Zn-equatorial ligand distances are 2.057(2) Å for Zn---O and 2.244(2) Å for Zn---N. The Zn---N distance for the apical imidazole ligands is 2.144(2) Å[29].

Hamed *et al.* [30] have reported that the compounds having the general formula:$K_n[M(FO)_2(H_2O)_2]\cdot xH_2O$, where (M = Cu(II) or Fe(III), n = 2 or 1 , FO = folate anion, x = 2 or 3 with respect) (Fig. 2.8), could be prepared and their absorption efficiency in rodent's blood was determined. The obtained compounds were characterized by elemental analysis, infrared as well as thermogravimetric analysis and polarization of light. The results suggest that the two folate complexes were formed in 1:2 molar ratio (metal:folic acid) which acted as a bidentate ligand through both carboxylic groups. Polarization of light proved that the folate complexes have symmetric geometry.

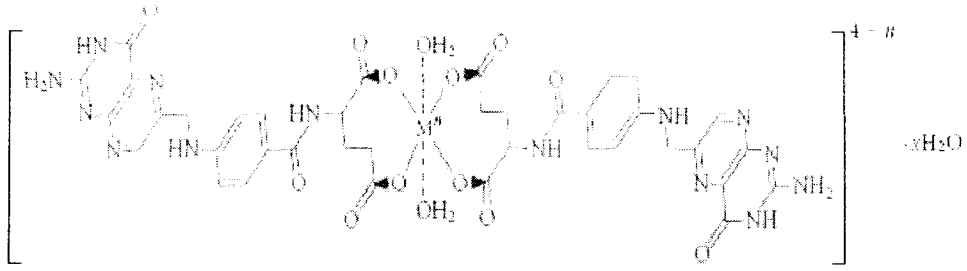

Fig. 2.8 Structure of $K_n[M(FO)_2(H_2O)_2] \cdot xH_2O$ [30].

V. M. Trukhan and his coworkers [31] have reported that the reaction of the new polydentate ligand 2,6-bis{3-[*N,N*-di(2-pyridylmethyl)amino]propoxy}benzoic acid (LH) with $Fe(ClO_4)_3$ followed by addition of chloroacetic acid leads to the formation of the tetranuclear complex $[\{Fe_2OL(ClCH_2\text{-}CO_2)_2\}_2](ClO_4)_4$ (Fig. 2.9), the crystal structure of which reveals that it consists of two $Fe^{II}_2(\mu\text{-}O)(\mu\text{-}RCO_2)_2$ cores linked *via* the two L ligands in a helical structure, with the carboxylate moieties of the two ligands forming a hydrogen-bonded pair at the center of the helix.

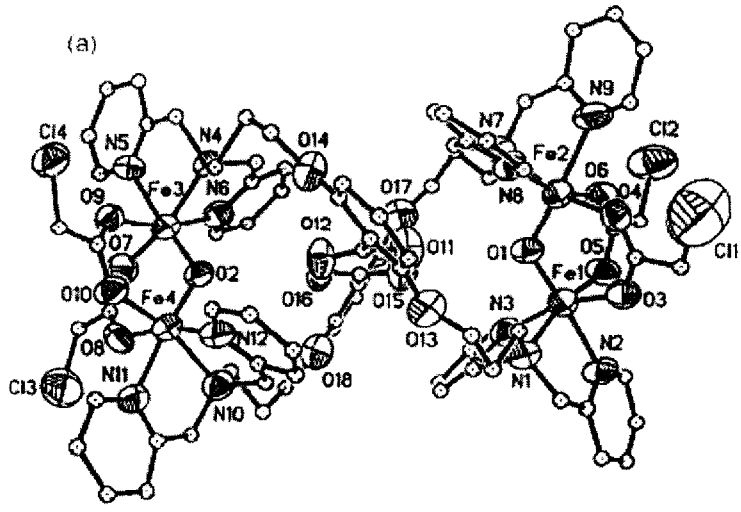

Fig. 2.9 Structure of $[\{Fe_2OL(ClCH_2\text{-}CO_2)_2\}_2](ClO_4)_4$ [31].

Ghattas *et al.* [32] prepared a μ-oxo-diiron(III) complex bridged by two molecules of 1-aminocyclopropane-1-carboxylic acid (ACCH) that was prepared with the ligand 1,4,7-triazacyclononane (TACN): $[(TACN)Fe_2(\mu\text{-}O)(\mu\text{-}ACCH)_2](ClO_4)_4 \cdot 2H_2O$ (**1**) (Fig. 2.10). This complex was characterized, and its crystal structure was

solved. The bridging amino acid moieties were found in their zwitterionic forms (noted as ACCH). Reactivity assays were performed in the presence of hydrogen peroxide and **1** turned out to be the first example of a well-characterized iron-ACCH complex able to produce ethylene from the bound ACCH moiety.

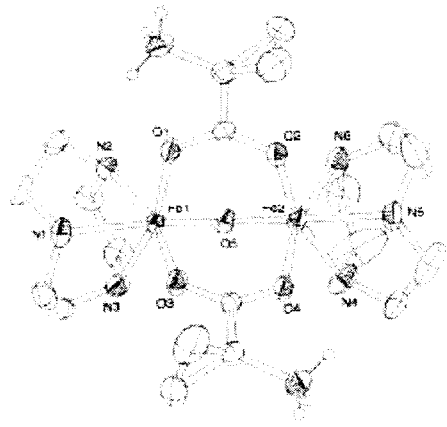

Fig. 2.10 Structure of the cation $[Fe_2(TACN)_2(\mu\text{-}O)(\mu\text{-}ACCH)_2]^{4+}$ [32].

C. M. Grant and his coworker [33] have carried out a reaction between $FeCl_3$, NaO_2CPh and L [L =1,2-bis(2,2′-bipyridyl-6-yl)ethane] in MeCN that gave the complex $[Fe_6O_4Cl_4(O_2CPh)_4L_2][FeCl_4]_2$ **1** whose cation contains an unusual $[Fe_6(\mu_3\text{-}O)_4]^{10+}$ core, whereas in MeOH the dinuclear complex $[Fe_2(OMe)_2Cl_2(O_2CPh)L][FeCl_4]$ **2** was obtained; magnetic studies indicate that the cations of **1** (Fig. 2.11) and **2** (Fig. 2.12) both have $S = 0$ ground states, consistent with the expected antiferromagnetic exchange interactions.

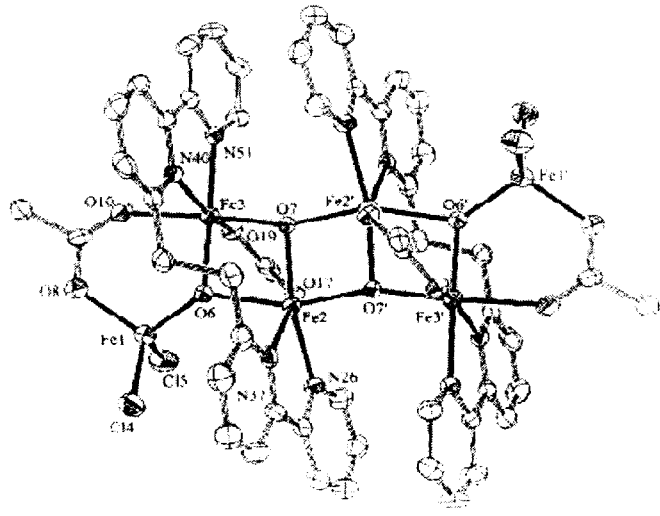

Fig. 2.11 Structure of the cation of **1** [33].

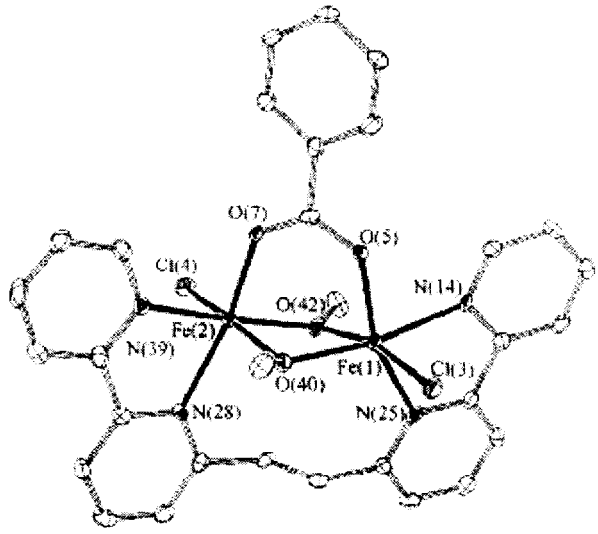

Fig. 2.12 Structure of the cation of **2** [33].

Moon *et al.* [34] have prepared the dinuclear Mn(II) complex, $[Mn_2(Hbida)_2(H_2O)_2]$ (Fig. 2.13), using a tetradentate tripodal ligand, *N*-(benzimidazol-2-ylmethyl)iminodiacetic acid (H_3bida) which has two carboxylate and one benzimidazole groups. The manganese ions are doubly bridged using μ,η^1-bridging monodentate carboxylate oxygen atoms. The Mn–Mn bond distance of 3.446 Å in this complex. The geometry of the complex is with four carboxylates in two different types of binding modes, non-bridging monodentate and μ,η^1-type bridging monodentate. The magnetic properties of the complex show a coupling constant of $J = -0.471(1)\ cm^{-1}$, which is consistent with weakly coupled antiferromagnetic Mn^{II} ($S = 5/2$) centers.

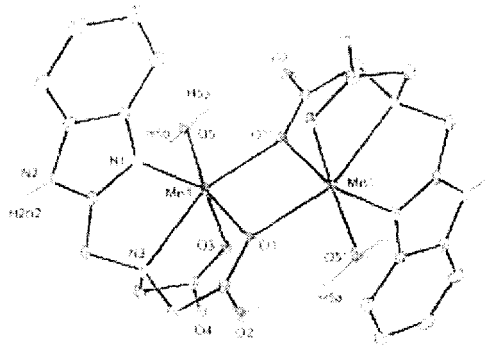

Fig. 2.13 The graphical structure of $[Mn_2(Hbida)_2(H_2O)_2]$ [34].

Maryudi *et al.* [35] have reported a method of synthesis of manganese carboxylates and their characterization. The new method involves reaction between molten carboxylic acid with sodium hydroxide in alcoholic solution to produce sodium carboxylates and continued by reacting sodium carboxylate with chloride salt of manganese. 1st and 2nd both step of reactions were conducted at 80-85°C and under perfect agitation. 2nd step of reaction took place well in the low concentration of manganese chloride, about 0.25 M or less. Thermogravimetric Analyzer test have been done and the results obtained in this study have exposed the capacity of manganese carboxylates stability at processing temperature of polyethylene.

Reaction of $Fe(O_2CCH_3)_2$ or $Mn(O_2CCH_3)_2.4H_2O$ with bidentate nitrogen donor ligands affords the trinuclear complexes $[M_3(O_2CCH_3)_6L_2]$ [M=Fe, L=BIPhMe **(1)** (Fig. 2.14); M= Mn, L=BIPhMe **(2)** (Fig. 2.15) or 1,10-phenanthroline **(3)]** in high yields. As judged from X-ray diffraction studies, these complexes adopt a novel linear structure, with one monodentate and two bidentate bridging carboxylates spanning each pair of metal atoms. Within this motif there are two geometric isomers that exist, designated "syn" or "anti" depending upon the orientation of the bidentate nitrogen donor ligands with respect to one another across the plane defined by the three metal atoms and the two monodentate bridging oxygen atoms. Structural characterization of three isomers of compound **2** revealed a considerable degree of flexibility in the tricarboxylate-bridged dimetallic unit, with M-M distances ranging from 3.370 (3) to 3.715 (2) Å [36].

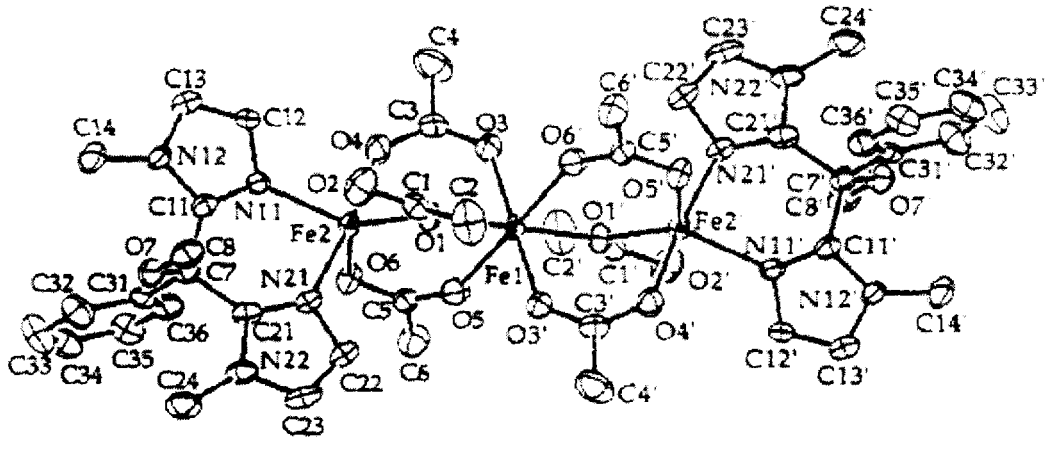

Fig. 2.14 Structure of $[Fe_3(O_2CCH_3)_6(BIPhMe)_2]\cdot 2THF$, *anti*-1[36].

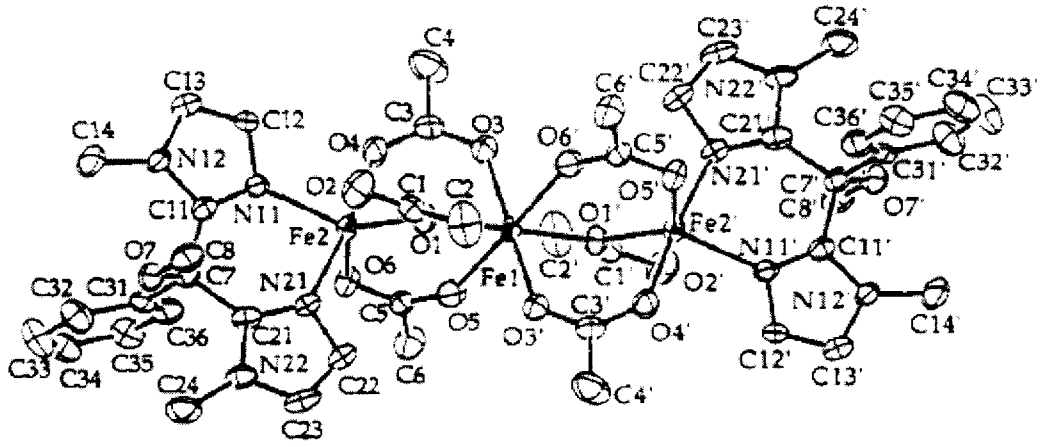

Fig. 2.15 Structure of $[Mn_3(O_2CCH_3)_6(BIPhMe)_2]\cdot 2CH_2Cl_2$, *anti*-2A [36].

Thermal decomposition of transition metal malonates, $MCH_2C_2O_4\cdot xH_2O$ and transition metal succinates, $M(CH_2)_2C_2O_4\cdot xH_2O$ (M=Mn, Fe, Co, Ni, Cu & Zn) have been studied employing TG, DTG, DTA, XRD, SEM, IR and Mössbauer spectroscopic techniques by Randhawa *et al.* [37]. After dehydration, the anhydrous metal malonates and succinates decomposed directly to their respective metal oxides in the temperature ranges 310-400°C and 400-525°C respectively. The oxides obtained have been found to be nanosized. The thermal stability of succinates was observed to be higher than that of the respective malonates [37].

Few complexes of Fe (III), Co (II), Ni (II) and Cu (II) with uracil, 6-amino uracil and those with substituted phenyl azo-6-amino uracils containing o-methyl,p-carboxy and o-carboxy subtituents and 5,5'-dietyl barbituric acid sodium salt have been synthesized and characterized by elemental analysis, magnetic moment and spectral measurements(IR, UV-Vis, ESR). The IR spectra showed that uracil existed in keto-enol tautomerism but 6-amino uracil possessed the kito amino–imine structure with some enol form. The iron complexes were with octahedral geometries. The square planar copper complexes existed in ligand bridged structures. The nickel complexes were of tetrahedral configuration. In general, the azo group was involved in the structural chemistry of the complexes. The coordination bond length was calculated. The thermal properties (TG and DTA) of the complexes were measured and discussed and thermodynamic parameters were also evaluated [38].

A. Golobič and his coworkers [39] applied different synthetic routes for preparation of some copper(II) carboxylates with 3-hydroxypyridine (3-pyOH). The monomeric and dimeric complex of copper(II) acetate were isolated, $[Cu(O_2CCH_3)_2(3\text{-}pyOH)_2]$, **1**, and $[Cu_2(O_2CCH_3)_4(3\text{-}pyOH)_2]$, **2**, respectively. A covalently linked 2D CuII compounds of general formula $[Cu(O_2CR)_2(3\text{-}pyOH)_2]_n$, were prepared with benzoate ($R=C_6H_5$, **3**), hexanoate ($R=CH_3(CH_2)_4$, **4**), and heptanoate ($R=CH_3(CH_2)_5$, **5**) ligands. The crystal structures of all five compounds were determined by X-ray structure analysis. The compounds were tested for fungicidal activity against two fungal species *Trametes versicolor* and *Antrodia vaillantii*. Complete growth retardation for *Antrodia vaillantii* was noticed for compounds **3**, **4**, and **5** at concentrations of $5 \cdot 10^{-3}$ mol L^{-1}, $1 \cdot 10^{-3}$ mol L^{-1}, and $5 \cdot 10^{-4}$ mol L^{-1}, while in the case of *Trametes versicolor* complete growth retardation was observed for the same three compounds only at the highest tested concentration.

Kozlevčar *et al.* [40] synthesized and characterized a series of compounds of the composition $[Cu_2(OOCC_nH_{2n+1})_4(nia)_2]$ (nia = nicotinamide; n = 6 to 11) and also tested for fungicidal activity. Crystal structure determinations revealed dinuclear structures of the copper(II) acetate hydrate type for compounds $[Cu_2(OOCC_6H_{13})_4(nia)_2]$-A (1A), $[Cu_2(OOCC_6H_{13})_4(nia)_2]$-B (1B) and $[Cu_2(OOCC_8H_{17})_4(nia)_2]$ (3). Other applied characterization methods indicate dimeric structures for all synthesized compounds [μ_{eff} (298 K) = 1.43–1.50 BM; characteristic band in UV-Vis spectra in the region λ = 350–400 nm]. The same conclusion may also be deduced from the IR ($\Delta = \nu_{asym}(COO^-) - \nu_{sym}(COO^-)$ = 183–189 cm^{-1}) and EPR spectra, though some differences were observed for heptanoate modification 1A, probably due to a different hydrogen bonding scheme. Screening for fungicidal activity against the wood-rotting fungus *Trametes versicolor* (L. ex Fr.) Pilat shows that the compounds dissolved in DMSO completely stop mycelium growth at a concentration of 1.0×10^{-3} mol L^{-1}. Some of them (n = 8, 9, 10) show strong activity also in more diluted solutions (1.0×10^{-4} mol L^{-1}).

S. Shahzadi and his coworkers [41] synthesized transition metal carboxylates, i.e., 3-[(2,4,6-trichloroanilino)carbonyl]prop–2-enoicacid and 3-[(4-bromoanilino) carbonyl] prop–2-enoic acid. The unimolar and bimolar substituted products have been characterized by elemental analysis, IR, UV-Vis spectroscopy, ^1H NMR, and

atomic absorption. IR data show the bidentate nature of the carboxylate group. The transition metal complexes were tested *in vitro* against a number of microorganisms to assess their biocidal properties.

2.3 Scope and objective

Carboxylates are ligands which contain O atoms as donors. In case of the dinitrobenzoic acid the nitro groups may also act as donors through the O and N atoms. Hence the acid as a ligand might be useful for complex formation. Therefore, the ligand was chosen to examine its complex forming ability with transition metals as a model and then to examine their fungitoxicity. Many transition metal compounds [39-43] are known to be potential fungicides.

2.4 Experimental

2.4.1 General Comments

The solvents used in reactions were of AR grade and were obtained from commercial sources (Merck, India). The solvents were dried using standard literature procedures. Water were distilled with sodium hydroxide and potassium permanganate where as methanol was distilled after reacting it with solid iodine and magnesium.

2.4.2 Materials

The 3,5-di nitro benzoic acid (s.d.fine-chem limited, India), $CuSO_4 \cdot 5H_2O$ (s.d.fine-chem limited, India), $CoCl_2 \cdot 6H_2O$ (Merck, India), $FeSO_4 \cdot 7H_2O$ (s.d.fine-chem limited, India), $ZnSO_4 \cdot 7H_2O$ (s.d.fine-chem limited, India), $MnCl_2 \cdot 4H_2O$ (Merck, India) of AR quality were used as received from commercial sources. Methanol (Merck, India) used in the reaction was of AR grade.

2.4.3 Measurements

The IR spectra in the range 4000-400 cm^{-1} were recorded on FTIR-8300 Shimadzu spectrophotometer with samples investigated with KBr on CsI window. UV/VIS spectra were recorded on JASCO V-530. Microanalyses were performed at

the ICAS, Kolkata, India. Magnetic susceptibility was measured at room temperature on a PAR 155 sample vibrating magnetometer using $Hg[Co(SCN)_4]$ as the calibrate. Differential calorimetric analyses were carried out on a Perkin-Elmer Thermal analyzer from 100-230°C at a heating rate of 10°C/min. Metals were estimated using standard methods in our laboratory.

2.4.4 Synthetic procedures

2.4.4.1 Preparation of sodium salt of 3,5-dinitro benzoic acid (LNa)

To a solution (40 ml) of 3,5-dinitro benzoic acid (4.0g, 18.85 mmol) was added drop wise with continuous stirring NaOH (0.75g, 18.85 mmol) solution in water (20 ml) in the presence of phenolphthalein as an indicator. The reaction system was stirred for half an hour. Solvents removed by evaporation, leaving behind the crystallized product of sodium salt of 3,5-dinitro benzoic acid. Then the sodium salt was further recrystallized in methanol and dried *in vacuo*.

LNa: Yield: 3.15 g; 78.75 %; M.P.: >240°C (dec).

Elemental analysis (Calcd. For $C_7H_3N_2O_6Na$):

Calcd.: C, 35.91; H, 1.29; N, 11.97 %.

Found: C, 35.82; H, 1.20; N, 11.94%.

IR (cm^{-1}): $\nu(OCO)_{asym}$, 1620(m); $\nu(OCO)_{sym}$, 1459 (s); $\nu(NO_2)_{asym}$, 1534(m); $\nu(NO_2)_{sym}$, 1345(m).

2.4.4.2 Preparation of Mn(II) complex of 3,5-dinitro benzoic acid (1)

Sodium salt of 3,5-dinitro benzoic acid (1.18g, 5.05 mmol) was dissolved in water (4 ml) methanol (120 ml) mixture and the solution was taken in 250 ml round bottomed flask. The $MnCl_2 \cdot 4H_2O$ (0.5g, 2.52 mmol) was dissolved in methanol (10 ml) and added drop wise to the sodium salt of the acid. The mixture was then heated under reflux for 10h. The brown volatiles were removed from reaction mixture and

the dry mass washed with hot methanol and the brownish solid of desired product was obtained by filtration which was dried *in vacuo*.

2.4.4.3 Preparation of Fe(II) complex of 3,5-dinitro benzoic acid (2)

Sodium salt of 3,5-dinitro benzoic acid (1.68g, 7.19 mmol) was dissolved in water (4 ml) methanol (130 ml) mixture and the solution was placed in 250 ml round bottomed flask. The $FeSO_4 \cdot 7H_2O$ (1.0g, 3.59 mmol) was dissolved in methanol (15 ml) and added drop wise to the sodium salt of the acid. The colour of the mixture turned to deep chocolate and a precipitate appeared. The mixture was heated under reflux for 6h. Desired product as a reddish brown precipitate was obtained by filtration. The product was washed with hot methanol and dried *in vacuo*.

2.4.4.4 Preparation of Co(II) complex of 3,5-dinitro benzoic acid (3)

Sodium salt of 3,5-dinitro benzoic acid (0.98g, 4.20 mmol) was dissolved in water (3 ml) methanol (140 ml) mixture and the solution was placed in 250 ml round bottomed flask. The $CoCl_2 \cdot 6H_2O$ (0.5g, 2.10 mmol) was dissolved in methanol (15 ml) and purple solution was added drop wise to the sodium salt of the acid. The colour of the mixture turned pink after addition was complete. The solution was then heated under reflux for 6h. Pink crystals of the desired product was obtained from the filtrate after 25 days on slow evaporation, at room temperature.

2.4.4.5 Preparation of Cu(II) complex of 3,5-dinitro benzoic acid (4)

Sodium salt of 3,5-dinitro benzoic acid (0.94g, 4.00 mmol) was dissolved in water (3 ml) methanol (130 ml) mixture and the solution was placed in 250 ml round bottomed flask. The $CuSO_4 \cdot 5H_2O$ (0.5g, 2.00 mmol) was dissolved in methanol (20 ml) and the blue solution was added drop wise to the sodium salt of the acid. After addition the colour of the mixture became intense blue. The solution was then heated under reflux for 6 h and then filtered. The filtrate was concentrated to a volume of 40 ml. Deep blue crystals of the desired product were obtained by slow cooling of the solution.

2.4.4.6 Preparation of Zn(II) complex of 3,5-dinitro benzoic acid (5)

Sodium salt of 3,5-dinitro benzoic acid (0.81g, 3.47 mmol) was dissolved in water (3 ml) methanol (120 ml) mixture and the solution was placed in a 250 ml round bottomed flask. The $ZnSO_4 \cdot 7H_2O$ (0.5g, 1.73 mmol) dissolved in methanol (15 ml) was added drop wise to the sodium salt of the acid. Then little amount of white precipitate was appeared. The mixture was the heated under reflux for 6h and then filtered. The filtrate was concentrated to a volume of 40 ml. White crystals of the desired product were obtained by slow cooling of the solution.

2.4.5 Crystal structure determinations

The crystals of **3** and **4** suitable for the X-ray diffraction study were prepared by slow crystallization of methanol solution of the respective compounds, the crystallographic analysis of compounds showed the sample had crystallized as methanol solvate. Intensity data were measured for selected crystals of **3** and **4** at 293 K on a Bruker SMART APEX diffractometer with fine-focus sealed graphite tube with MoKα radiation, λ= 0.71073 Å so that θ_{max} = 27.5°. The data set was corrected for absorption based on multiple scans [44]. Each structure was solved by SHELXS-97 [45] and refined by a full-matrix least-squares procedure SHELXL-97 [45] on F^2 with primary atom site location: structure- invariant direct methods, with hydrogen atoms treated by a mixture of independent and constrained refinement and using a weighting scheme of the form $w= 1/[\sigma^2(F_o^2)+ (0.0522P)^2 + 0.1427P]$ where $P = (F_o^2 + 2F_c^2)/3$. For compound **3** carbon-bound H-atoms were placed in calculated positions (C–H 0.93 to 0.96 Å) and were included in the refinement in the riding model approximation, with *U*iso(H) set to 1.2 to 1.5 *U*equiv(C). The methanol H-atoms were located in a difference Fourier map, and were refined with a distance restraint of O–H 0.85±0.01 Å; their *U*iso values were freely refined. The molecular structures showing crystallographic numbering schemes were drawn with 50% displacement ellipsoids using ORTEP-3 [46] and diagrams were generated with the aid of the DIAMOND programmer [47].

2.4.6 Crystallographic data and refinement details for 3 and 4

Crystallographic data and refinement details for **3**

Formula	$[Co\ (C_7H_3N_2O_6)_2\ (CH_3OH)_4]$
Formula weight	609.33
Crystal habit, colour	Prism, pink
Ctystal system	Triclinic
Space group	$P\bar{1}$
a (Å)	6.4068(8)
b (Å)	8.7660(11)
c (Å)	12.1603(16)
α (°)	90.411(2)
β (°)	100.407(2)
γ (°)	102.214(2)
V ($Å^3$)	655.77(14)
Z	1
D_x ($Mg\ m^{-3}$)	1.543
λ(MoKα, Å)	0.71073
F(000)	313
Crystal size (mm)	0.35 × 0.30 × 0.05
Absorption coefficient μ (mm^{-1})	0.74
θ range for data collection (°)	2.4-22.8
Reflection collected	6372
Independent reflection	2999
R_{int}	0.028
Reflection with $I > 2\sigma(I)$	2388
Number of parameters	188
$R[F^2 > 2\sigma(F^2)]$	0.043
$wR(F^2)$	0.110
S	1.03
Largest difference peak and hole ($Å^{-3}$)	0.001,0.38

2.4.7 Biological studies

2.4.7.1 Antifungal activity

The virulent fungal strains of *Lasiodiplodia theobromae* and *Cruvularia eragrostidis* were collected from the type culture collection, Dr. A. Saha, Depertment of Botany, University of North Bengal. The strains were isolated from *L. theobromae* (a pathogen of mango, *Magnifera indica*) and *C. eragrostidis* (a pathogen of tea, *Camellia sinensis*). These strains were grown on potato- dextrose agar (PDA, HiMedia, India) medium at 27°C. The fungicidal activities were determined following spore germination bioassay as described by Rouxel *et al.*[48]. Purified eluants (15µl) were placed on two spots 3 cm apart on a clean grooved slide. One drop of spore suspension (15µl), which was prepared from 15 day old cultures of the fungi, was added to the treated spots. The slides were incubated in trays at 27°C for 24h under humid conditions. After incubation, one drop of Lactophenol mixture was added to each spot to fix the germinated spores. The number of spore germination events was compared with the spore germination of the control.

2.4.7.2 Phytototoxic effect

Seeds of Indian rice (*Oryzae sativa*), *cultivar Khitish* were collected from the Directorate of Farm, Uttar Banga Krishi Viswavidyalaya, Cooch Behar, West Bengal, India. Seeds were first surface sterilized with 0.1% mercuric chloride for 3 min, washed with distilled water and then the phytotoxic effects of the transition metal carboxylates (dissolved in 2 ml methanol then diluted with 10 ml water) were determined [49]. Seeds were incubated with different concentration of transition metal carboxylates for different time periods. After incubation, the seeds were washed with distilled water and incubated in a B.O.D. incubator for 48h at 27°C. The percentage of seed germination was calculated and compared with the control.

2.5 Result and discussion

2.5.1 Preparation of sodium salt of 3,5-dinitrobenzoic acid

Sodium salt of the 3,5-dinitrobenzoic acid was prepared by neutralization with equimolar aquous solution of sodium hydroxide. The sodium salt of the 3,5-

dinitrobenzoic acid was obtained in good yield. The product was recrystallized from water/ethanol mixture. The ligand was soluble in water, water/ethanol and water/methanol mixture. The ligand had a decomposition temperature at > 240°C. The synthetic detail and characterization data for LH and LNa are described in section 2.4.4.1. The formula of the ligand and the abbreviations of the complexes are presented in scheme 2.1.

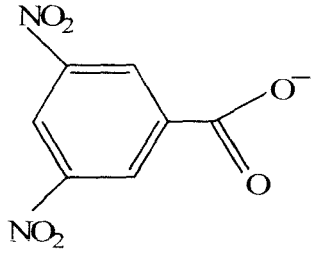

1. $[Mn(L)_2.(CH_3OH)_4]$; **2.** $[Fe(L)_2.(CH_3OH)_4]$; **3.** $[Co(L)_2.(CH_3OH)_4]$;

4. $[Cu_2(L)_4 \cdot Cu(L)_2 \cdot (CH_3OH)]$; **5.** $[Zn(L)_2.(CH_3OH)_4]$

Scheme 2.1

2.5.2. Synthesis of transition metal(II) complexes of 3,5-dinitrobenzoic acid (LH)

The transition metal carboxylates of 3,5-dinitrobenzoic acid (M=Mn, Fe, Co, Cu and Zn) were obtained in moderate yields (except for Mn-carboxylate) by the 1:2 reaction of transition metal sulfates/chlorides with the sodium salt of the ligand in water/methanol mixture as solvent for refluxation (Eq. 1 and Eq. 2) . The sodium salt of the ligand was generated by the addition of aqua's solution of NaOH to the aquous solution of 3,5-dinitrobenzoic acid. The reactions were completed in 10h time. The complexes produced are neutral chelated types. These are air stable for 48h because bonding solvents are released. The synthetic methodologies are described in scheme 2.2.

$$LH + NaOH \longrightarrow LNa + H_2O \quad .....(1)$$

$$LNa + MCl_2/MSO_4 \longrightarrow M(L)_2 + NaCl/Na_2SO_4 \quad .....(2)$$

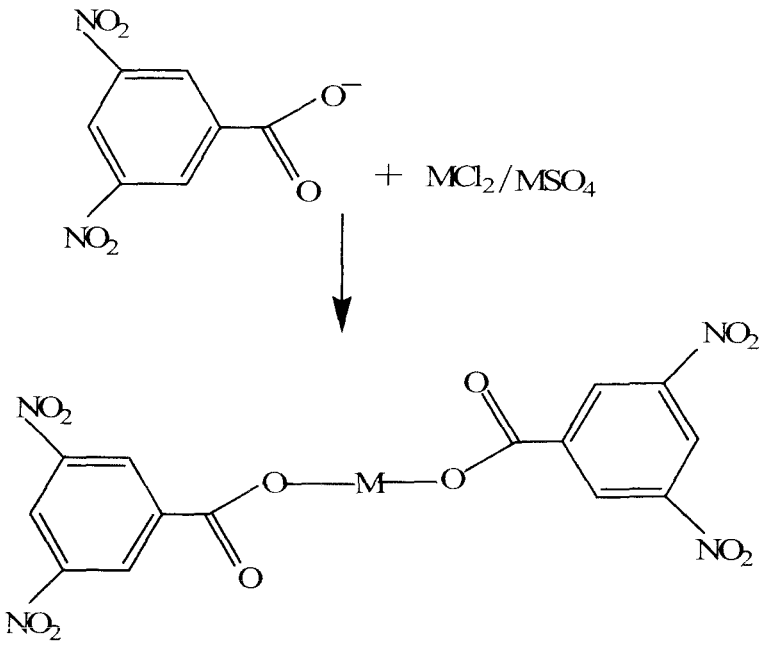

1. [$Mn(L)_2(CH_3OH)_4$]; **2.** [$Fe(L)_2(CH_3OH)_4$]; **3.** [$Co(L)_2(CH_3OH)_4$];

4. [$Cu_2(L)_4 . Cu(L)_2 \cdot (CH_3OH)$]; **5.** [$Zn(L)_2(CH_3OH)_4$]

Scheme 2.2

2.5.3 Spectroscopic characterization and X-ray crystal structure determination of transition metal carboxylates, $M(L)_2$ [where M= Mn, Fe, Co, Cu and Zn; L=3,5-dinitrobenzoic acid]

The complexes were characterized by UV, IR and elemental analysis Magnetic moment data further suggested the composition of the complexes as proposed. The composition of the complexes, however, are mainly based upon the elemental analyses supported by the spectroscopic and other data where available as far as practicable in our laboratory conditions. In general, the X-ray crystallographic data of the complexes *(e.g.*,**3** and **4**) supports the observed spectral and magnetic moment data. Table 2.1 contains the relevant physical data of the compounds.

Table 2.1. Physical and analytical data for **1-5.**

Composition	Yield(%)	M.P.(°C)	Colour	Elemental composition found (calcd) (%)			
				C	H	N	M
1. $[Mn(C_7H_3N_2O_6)_2 \cdot (CH_3OH)_4]$	30	Started decomposing at >230°C	Pale-brown	35.48 (35.72)	3.62 (3.66)	9.22 (9.26)	8.99 (9.08)
2. $[Fe(C_7H_3N_2O_6)_2 \cdot (CH_3OH)_4]$	87	172-174	Brown	35.75 (35.66)	3.58 (3.66)	9.20 (9.24)	9.11 (9.21)
3. $[Co(C_7H_3N_2O_6)_2 \cdot (CH_3OH)_4]$	85	Started decomposing at 129°C	Pink	35.31 (35.48)	3.72 (3.63)	9.11 (9.19)	9.73 (9.67)
4. $[Cu_2(C_7H_3N_2O_6)_4 \cdot Cu(C_7H_3N_2O_6)_2 \cdot (CH_3OH)]$	80	Started decomposing at 218°C	Deep blue	34.68 (34.50)	1.49 (1.38)	11.29 (11.15)	12.80 (12.69)
5. $[Zn(C_7H_3N_2O_6)_2 \cdot (CH_3OH)_4]$	75	165-167	White	35.01 (35.11)	3.48 (3.60)	9.05 (9.10)	10.45 (10.62)

2.5.3.1 IR spectra

Selected IR spectra and their assignment for the transition metal carboxylates have been presented in Table 2.2. A broad band in the 3500-3200cm^{-1} region is assigned to -OH stretching modes. The carboxylate group displayed two absorbance bands one at $\nu(OCO)_{asym}$ 1630-1660 cm^{-1} region and other at $\nu(OCO)_{sym}$ 1400-1470 cm^{-1} region in the complexes [50]. The nitro group also displayed two absorbance bands. The $\nu(NO_2)_{asym}$ and $\nu(NO_2)_{sym}$ bands appeared at 1527-1545 cm^{-1} and at 1340-1357 cm^{-1} respectively in the transition metal complexes [50]. The broad band at 3500-3200 cm^{-1} due to ν(OH) attributable to the coordinated methanol (solvent) molecules slowly disappeared as the solvent molecules were lost during standing the complexes at room tempareture on bench for ~ 48h. This indicated that the solvent molecules are loosely bound to the central metal atom. The carboxylate stretching

frequency indicated it to be a bridging bidentate type rather than a monodentate type. The difference between $\nu(OCO)_{asym}$ and $\nu(OCO)_{sym}$ ($\Delta\nu$= 153-166) is an indication of the bridging nature of the ligand [51]. Crystallographic data also confirmed the IR spectral interpretation at least for two complexes (**3** and **4**). The IR of the Cu-carboxylate compound (**4**) attracts special interest. The structure has a dimeric Cu_2 unit as well as a monomeric carboxylate molecule in its molecule joined via a $NO_2\cdots O$ (Fig. 2.18). The IR stretching vibrations for the –OCO group, therefore, show two types of absorptions both are in the same frequency range but identifiably separate. The one binding the single Cu(II) units as a bridging bidentate group, the other also as the bridging bidentate group but bridging the Cu atoms in the Cu_2 dimeric moiety.

The complexation of the carboxylate moiety to the metal atom is indicated in the new compounds not only by the x-ray crystal structure determinations (for Co^{2+} and Cu^{2+}) but also by the shift of νCO of the (free) carboxylic acid group(-COOH) at 1699cm^{-1} to the ~1622-1629 cm^{-1} $\nu(OCO)_{asym}$ and ~1458-1469cm^{-1} $\nu(OCO)_{sym}$. In addition, the $\nu(NO_2)_{asym}$ and $\nu(NO_2)_{sym}$ of the ligand molecule could be assigned unequivocally.

The shape of the $\nu(NO_2)$ band in the spectra merits a point to be mentioned. The band is strong and slightly broad which on closer inspection indicates that an additional stretching frequency is present almost superimposed on it. This additional band is most likely due to the $\nu(NO_2)$ of the coordinated -NO_2 group. The -NO_2 group is connected to form the molecule of the complex with a "Cu-carboxylate dimer" and a mononuclear species... which are not connected via bridging carboxylate ligands but via the nitro-O atoms... as has been demonstrated by the X-ray crystallography (Fig. 2.18). In all other compounds of this series -NO_2 group stretching frequency did not show this characteristic indicating its noninvolvement in further coordination.

2.5.3.2 Magnetic moment

The magnetic moment data are in table 2.3. The magnetic moment data indicate an octahedral geometry for Mn(II), Fe(II) and Co(II) complexes. The magnetic moment data correspond satisfactorily to the required values for unpaired electrons in the compounds for an octahedral disposition around the central metal ion

[52]. The subnormal value of μ_{eff} for Cu(II) complex indicates that the coordination is possibly octahedral around the metal atom and suggesting an antiferromagnetic spin-exchange interaction within each molecule [53]. The magnetic moment data thus indicates in the complex a dimeric Cu_2 unit is present. The magnetic moment value of 1.49 B.M. per copper appears to be low for a d^9 configuration. This suggests the presence of a strong spin-spin interaction through the bridging ligand in the dimeric unit [54-58] as also identified by the preliminary X-ray crystallography study.

Table 2.2 IR spectral data (cm^{-1}) for compounds **1-5**

Compound	$\nu(OCO)_{asym}$	$\nu(OCO)_{sym}$	$\Delta\nu = [\nu(OCO)_{asym} - \nu(OCO)_{sym}]$	$\nu(OH)$	$\nu(NO_2)_{asym}$	$\nu(NO_2)_{sym}$
1.	1624(s)	1460(s)	164	3446(v,b)	1541(s)	1350(s)
2.	1624(m)	1458(s)	166	3421(m,b)	1541(s)	1352(s)
3.	1627(w)	1462(m)	165	3386(m,b)	1527(w)	1357(s)
4.	1629(m) [a]1655(s)	1467(s) [a]1400(s)	162	3356(w,b)	1536(m) [b]1545(s)	1355(s) [b]1340(s)
5.	1622(m)	1469(m)	153	3421(v,b)	1542(m)	1344(s)

s, strong; m, medium; w, weak; b, broad; v, very

a= weak bridging bidentate type $\nu(OCO)$, b=For uncoordinated free $\nu(NO_2)$

2.5.3.3 Differential calorimetric analysis

The Differential calorimetric analysis of **2** exhibited a peak at 171.56°C. It shows that the enthalpy at 171.56°C is ΔH =14.11 J/g. The complexes **3** and **4** on heating from 100-230°C underwent decomposition. The compound **3** displayed a peak at 128.64°C corresponding to the melting of the compound (ΔH =10.38 J/g). Compound **3** after melting yielded a compound which underwent further decomposition between 130-150°C. Compound **3** decomposes further beyond 150°C finally to decompose at 163.93°C (ΔH =74.12 J/g). The compound **4** also underwent decomposition at a temperature between 148.07°C to 218.56°C. At 218.56°C the enthalpy of **4** was (ΔH =50.31 J/g). But no information of phase change could be

obtained during the cooling of the compounds as because the compounds were decomposed by then. It is likely that the compounds decomposed by giving off CO_2. However, investigations on the decomposed products were not carried out in this investigation.

2.5.3.4 Electronic Spectra

The spectral data for **1–5** are summarized in Table 2.4. Towards the visible region, the electronic spectra showed absorptions for **3** and **4** attributable to an $n \rightarrow \pi^*$ transition within the nitro group and benzene ring chromophore owing to extensive conjugation, which is most likely the reason for the observed spectra in methanol solution.

Table 2.3 Magnetic moment data for compounds **1-4**[a]

Complex	Magnetic moment (B.M.)	No. of unpaired spins	Hybridization	Stereochemistry
1.	5.88	5	d^2sp^3	Octahedral
2.	4.99	4	d^2sp^3	Octahedral
3.	4.48	3	d^2sp^3	Octahedral
4.	1.49	1	sp^3d^2	Octahedral

[a] $Hg[Co(SCN)_4]$ as standard

Table 2.4 Electronic absorption spectra of compounds **1-5** recorded in methanol

Compounds	λ_{max}(nm)
1.	234,209
2.	229,214
3.	236,222, 515
4.	234, 214, 458
5.	232,213

2.5.3.5 X-ray Crystal Structure

This section deals with the X-ray crystallographic studies of transition metal carboxylates of 3,5-dinitrobenzoic acid Co(II) and Cu(II). Compounds **3** and **4** provided single crystals suitable for the X-ray crystal structure determination. The crystal structures of these complexes are described below.

2.5.3.5.1 Crystal Structure of Co(II) complex of 3,5-dinitrobenzoic acid (3)

The author was able to successfully isolate suitable single crystal of **3** for X-ray crystallography. The Co^{II} atom (site symmetry $\bar{1}$) in the title complex, $[Co(C_7H_3N_2O_6)_2(CH_3OH)_4]$, exists within an octahedral O_6 donor set defined by two *O*-monodentate 3,5-dinitrobenzoate anions and four methanol O atoms. An intramolecular O_m–H· · ·O_c (m = methanol and c = carbonyl) hydrogen bond leads to the formation of an *S*(6) ring. In the crystal, centrosymmetrically related molecules associate via further O_m–H· · ·O_c hydrogen bonds, leading to linear supramolecular chains propagating along the a-axis direction. The Co(II) atom in (I), (Fig. 2.16), is located on a crystallographic centre of inversion and exists within an octahedral O_6 donor set defined by two carboxylate-O1 atoms and four methanol-O atoms. The Co–O1 bond distance [Co–O1 = 2.0666 (17) Å] is comparable to those, *i.e.* 2.0525 (20) and 2.0587 (19) Å, found in the related tetra-aqua-bis(3,5-dinitrobenzoato-*O*)cobalt(II) tetrahydrate structure [59-61]. A small disparity in the Co—$O_{methanol}$ bond distances in (I) [Co–O7 = 2.1094 (16) and Co–O8 = 2.0645 (18) Å] is noted. The methanol-O7–H hydrogen forms an intramolecular O–H···O hydrogen bond with the carbonyl-O2 atom to close an almost planar {Co–O–C–O···H–O} S(6) ring, Table 2.5. The methanol-O8–H also forms a hydrogen bond to the carbonyl-O2 atom on a centrosymmetrically related complex, Table 2.5. This results in the formation of 12-membered $\{Co–O–H···O–C–O\}_2$ synthons and linear supramolecular chains along the *a* axis, (Fig. 2.17).It is noted that the packing of molecules brings into close proximity two nitro-O atoms, i.e. O4···$O4^{ii}$ = 2.756 (3) Å for 3-*x*, -*y*, 2-*z*. While the nature of this interaction is not obvious, there are approximately 50 precedents for such O_{nitro}···O_{nitro} contacts < 2.70 Å in the crystallographic literature [62]. Table 2.6 describes the Hydrogen-bond geometry in (Å, °) and Geometric parameters (Å, °) is presented below.

Table 2.5 Selected bond lengths (Å).

Compound	**3**
Co—O7	2.1094 (16)
Co—O8	2.0666 (17)
Co—O1	2.0666 (17)

Table 2.6 Hydrogen-bond geometry (Å, °) of compound **3**.

D—H···*A*	*D*—H	H···*A*	*D*···*A*	*D*—H···*A*
O7—H7o···O2^{i}	0.85 (3)	1.840 (15)	2.645 (2)	158 (3)
O8—H8o···O2^{ii}	0.85 (3)	1.817 (10)	2.662 (2)	179 (3)

Symmetry codes: (i) $-x+1, -y+1, -z+1$; (ii) $x-1, y, z$.

Geometric parameters (Å, °) of compound **3**.

Co—O8	2.0645 (18)	N2—C6	1.476 (4)
Co—O8^{i}	2.0645 (18)	C1—C2	1.511 (3)
Co—O1	2.0666 (17)	C2—C7	1.380 (3)
Co—O1^{i}	2.0666 (16)	C2—C3	1.385 (3)
Co—O7	2.1094 (16)	C3—C4	1.373 (3)
Co—O7^{i}	2.1094 (16)	C3—H3	0.9300
O1—C1	1.250 (3)	C4—C5	1.371 (4)
O2—C1	1.247 (3)	C5—C6	1.378 (4)
O3—N1	1.179 (4)	C5—H5	0.9300
O4—N1	1.190 (3)	C6—C7	1.379 (4)
O5—N2	1.220 (4)	C7—H7	0.9300
O6—N2	1.209 (4)	C8—H8A	0.9600
O7—C8	1.418 (3)	C8—H8B	0.9600
O7—H7O	0.85 (3)	C8—H8C	0.9600
O8—C9	1.408 (3)	C9—H9A	0.9600
O8—H8O	0.85 (3)	C9—H9B	0.9600
N1—C4	1.482 (3)	C9—H9C	0.9600
O8—Co—O1	91.36 (8)	C7—C2—C3	119.3 (2)
O8i—Co—O1	88.64 (8)	C7—C2—C1	120.5 (2)
O8—Co—O1^{i}	88.64 (8)	C3—C2—C1	120.2 (2)
O8i—Co—O1^{i}	91.36 (8)	C4—C3—C2	119.1 (2)
O8—Co—O7	88.14 (7)	C4—C3—H3	120.5
O8i—Co—O7	91.86 (7)	C2—C3—H3	120.5
O1—Co—O7	89.22 (7)	C5—C4—C3	123.3 (2)
O1i—Co—O7	90.78 (7)	C5—C4—N1	119.3 (2)
O8—Co—O7i	91.86 (7)	C3—C4—N1	117.4 (2)
O8i—Co—O7i	88.14 (7)	C4—C5—C6	116.3 (2)
O1—Co—O7i	90.78 (7)	C4—C5—H5	121.9
O1i—Co—O7i	89.22 (7)	C6—C5—H5	121.9
O1—Co—O1i	180.0	C5—C6—C7	122.6 (2)
O7—Co—O7i	180.0	C5—C6—N2	119.1 (3)
O8—Co—O8i	180.0	C7—C6—N2	118.3 (3)
C1—O1—Co	130.70 (16)	C6—C7—C2	119.4 (2)
C8—O7—Co	128.82 (16)	C6—C7—H7	120.3

C8—O7—H7O	113 (2)	C2—C7—H7	120.3
Co—O7—H7O	105 (2)	O7—C8—H8A	109.5
C9—O8—Co	131.57 (18)	O7—C8—H8B	109.5
C9—O8—H8O	110 (2)	H8A—C8—H8B	109.5
Co—O8—H8O	118 (2)	O7—C8—H8C	109.5
O3—N1—O4	122.3 (3)	H8A—C8—H8C	109.5
O3—N1—C4	118.6 (3)	H8B—C8—H8C	109.5
O4—N1—C4	119.1 (3)	O8—C9—H9A	109.5
O6—N2—O5	123.7 (3)	O8—C9—H9B	109.5
O6—N2—C6	118.5 (3)	H9A—C9—H9B	109.5
O5—N2—C6	117.8 (3)	O8—C9—H9C	109.5
O2—C1—O1	126.1 (2)	H9A—C9—H9C	109.5
O2—C1—C2	118.0 (2)	H9B—C9—H9C	109.5
O1—C1—C2	115.9 (2)		
O8—Co—O1—C1	87.5 (2)	C1—C2—C3—C4	−179.8 (2)
O8i—Co—O1—C1	−92.5 (2)	C2—C3—C4—C	5 0.0 (4)
O7—Co—O1—C1	175.6 (2)	C2—C3—C4—N1	179.5 (2)
O7i—Co—O1—C1	−4.4 (2)	O3—N1—C4—C5	173.0 (3)
O8—Co—O7—C8	125.9 (2)	O4—N1—C4—C5	−9.2 (5)
O8i—Co—O7—C8	−54.1 (2)	O3—N1—C4—C3	−6.5 (5)
O1—Co—O7—C8	34.5 (2)	O4—N1—C4—C3	171.2 (3)
O1i—Co—O7—C8	−145.5 (2)	C3—C4—C5—C6	0.2 (4)
O1—Co—O8—C9	−58.0 (3)	N1—C4—C5—C6	−179.3 (3)
O1i—Co—O8—C9	122.0 (3)	C4—C5—C6—C7	−0.5 (4)
O7—Co—O8—C9	−147.1 (3)	C4—C5—C6—N2	178.2 (3)
O7i—Co—O8—C9	32.9 (3)	O6—N2—C6—C5	177.2 (3)
Co—O1—C1—O2	−6.2 (4)	O5—N2—C6—C5	−3.4 (5)
Co—O1—C1—C2	175.42 (15)	O6—N2—C6—C7	−4.0 (5)
O2—C1—C2—C7	−178.2 (2)	O5—N2—C6—C7	175.4 (3)
O1—C1—C2—C7	0.3 (4)	C5—C6—C7—C2	0.6 (4)
O2—C1—C2—C3	1.6 (4)	N2—C6—C7—C2	−178.1 (3)
O1—C1—C2—C3	−179.9 (2)	C3—C2—C7—C6	−0.3 (4)
C7—C2—C3—C4	0.0 (4)	C1—C2—C7—C6	179.5 (2)

Symmetry codes: (i) $-x+1, -y+1, -z+1$.

Supplementary data and figures for this paper are available from the IUCr electronic archives (Reference: HB5347).

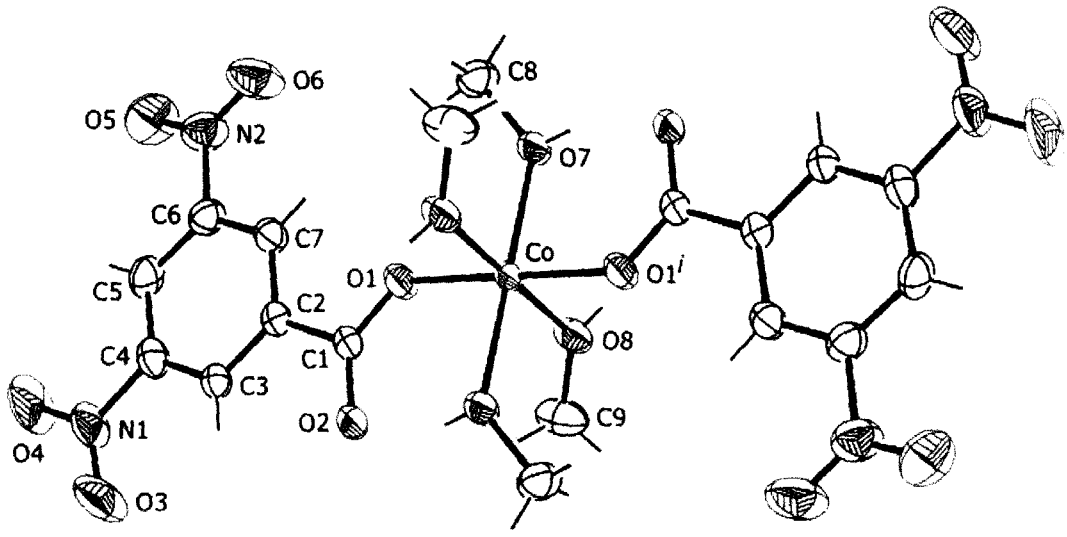

Fig. 2.16 The molecular structure of (**3**) extended to show the coordination geometry for the Co(II) atom, showing displacement ellipsoids at the 50% probability level. Symmetry operation*i*: 1-*x*, 1-*y*, 1-*z*.

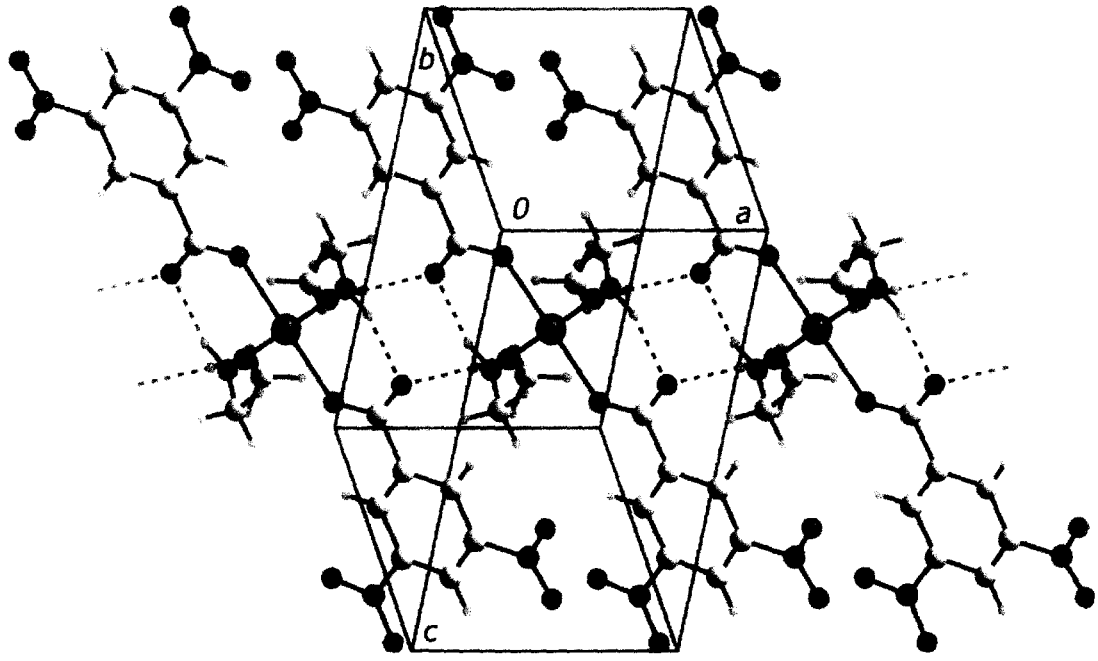

Fig. 2.17 Linear supramolecular chain along the *a* axis in (**3**) mediated by O—H···O hydrogen bonding. These and the intramolecular O–H···O hydrogen bonds are shown as blue dashed lines.

2.5.3.5.1 Crystal Structure of Cu(II) complex of 3,5-dinitrobenzoic acid (4)

The author was able to successfully isolate suitable single crystals of **4** for X-ray crystallography. The preliminary analysis of the X-ray crystallography studies of **4** reveals that the complex contains the asymmetric unit comprises two Cu centers, three carboxylates, a coordinated methanol molecule and half a solvent methanol molecule. These connect to form a "Cu carboxylate dimer" and a mononuclear species which are connected via bridging carboxylate ligands but via the nitro-O atoms (Fig. 2.18) and overall, a 2-D array is formed (Fig. 2.19). The details of the bond angles and bond distances are not available at the moment.

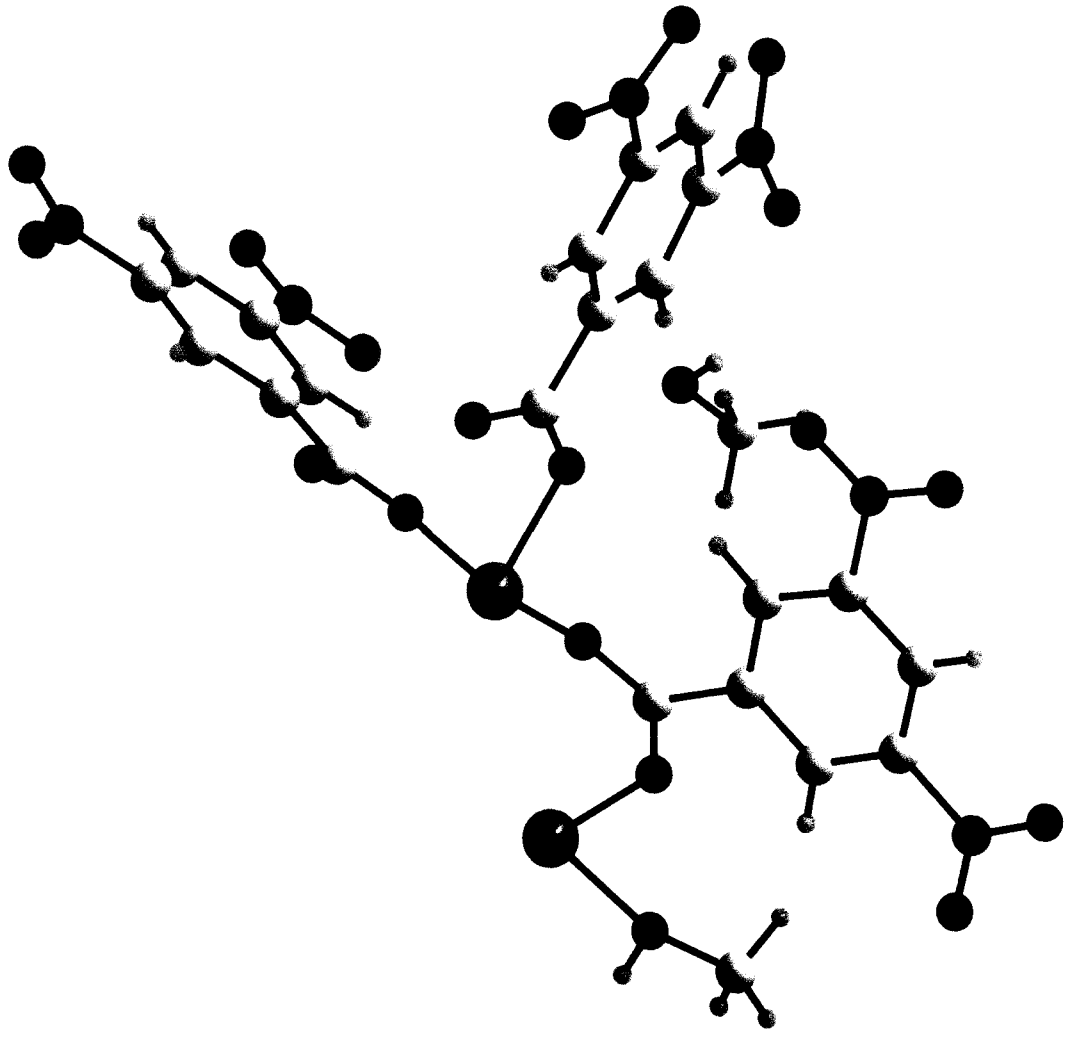

Fig. 2.18 X-ray crystallography structure of the asymmetric unit of compound **4**.

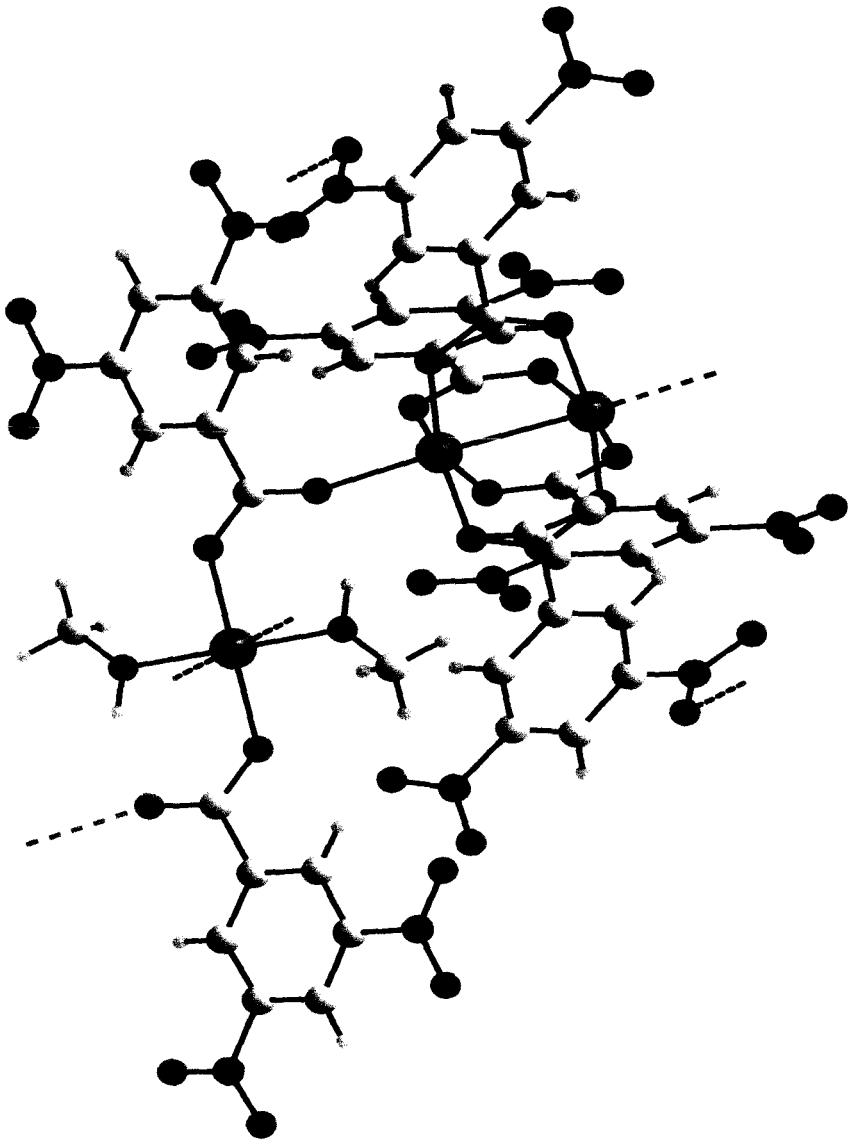

Fig. 2.19 A 2-D array of compound **4**.

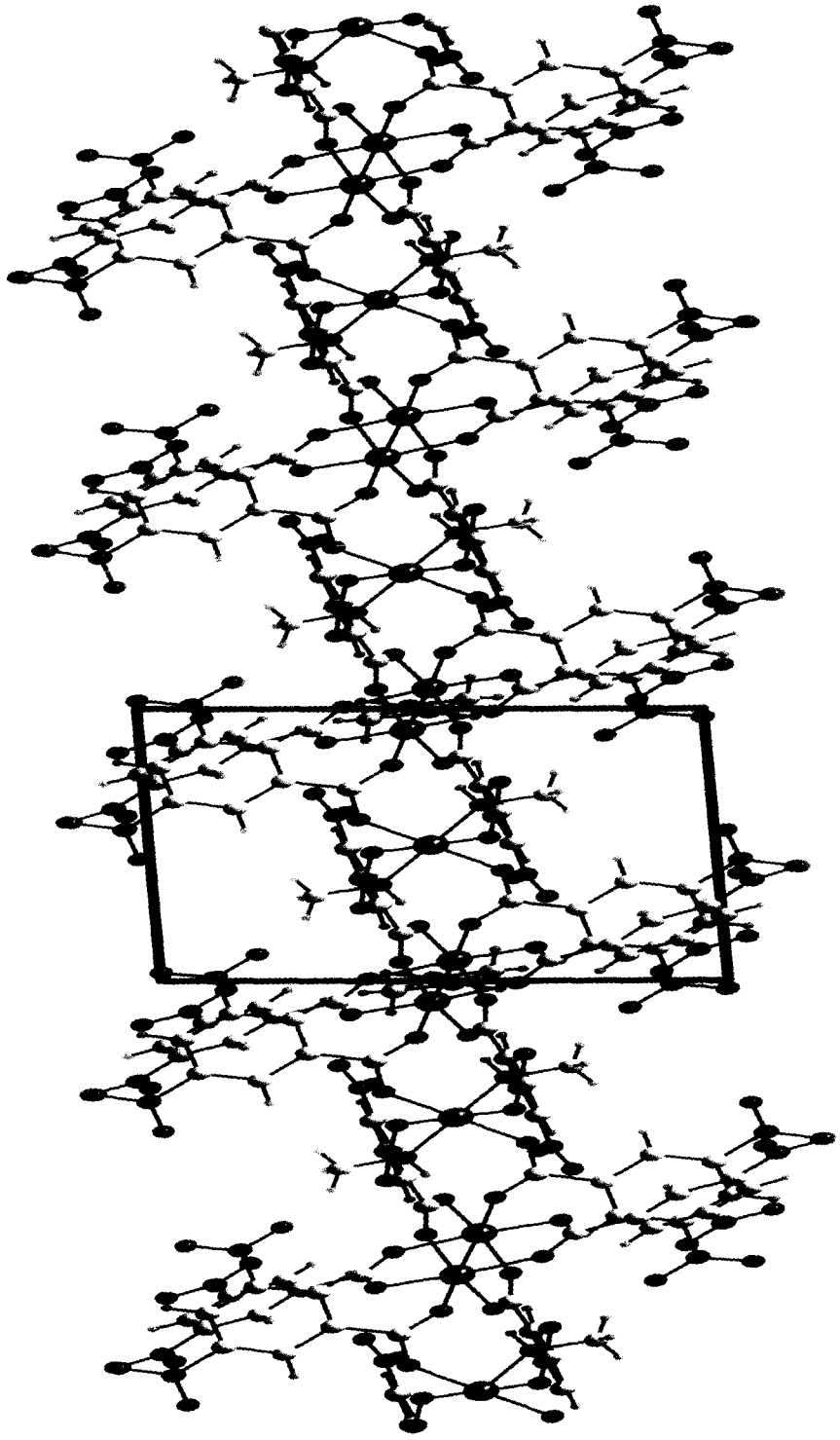

Fig. 2.20 Crystal packing structure of compound **4**.

2.5.4 Biological properties of transition metal carboxylates of 3,5-dinitrobenzoic acid.

2.5.4.1 Anti-fungal activities

The antifungal properties of the transition metal carboxylates **2-4** are summarized in table 2.5. The fungitoxic effect of the transition metal carboxylates were screened at three concentrations 25, 50 and 100 ppm, on spore germination of two different pathogens of mango (*L. theobromae*) and tea (*C. eragrostidis*). The results showed that **4** was most active followed by **3** against the tested fungal strains. Copper fungicides in potentiality are comparable to organtin compounds, such as triphenyltin acetate and triphenyltin hydroxide [63]. The compound **4** markedly inhibit the spore germination of each of the above fungi at concentrations above 50 ppm. At 100 ppm, almost complete inhibition of spore germination ensued, irrespective of the pathogen, which indicates high fungitoxicity against different groups of pathogen.

Table 2.5. Spore germination (%) of *L. theobromae* and *C. eragrostidis* in the presence of compounds **2–4**.

Chemicals	Spore germination % of *L. theobromae*.			Spore germination % of *C. eragrostidis*.		
	Conc (ppm)			Conc (ppm)		
	25	50	100	25	50	100
2.	84.0	78.5	68.3	86.6	79.2	67.1
3.	81.2	49.3	23.4	79.3	48.3	21.4
4.	14.1	5.1	2.2	12.2	5.7	2.5
Control (water)	87			92		

2.5.4.2 Phytotoxic properties

The phytotoxic effects of transition metal carboxylates were studied on economically important crop *Oryzae sativa* (Khitish). The phytotoxic effects of compounds **2–4** as a function of the concentration are summarized in Table 2.6. The results indicate that none of the transition metal carboxylates displays any inhibitory effect on seed germination.

Table 2.6 Phytotoxicity of compounds **2–4**, after seed treatment of Indian rice (*Oryzae sativa*), cultivar Khitish.

Compound	Percentage (%) of seed germination after 4h treatment			Percentage (%) of seed germination after 8h treatment			Percentage (%) of seed germination after 12h treatment		
	Conc. (ppm)			Conc. (ppm)			Conc. (ppm)		
	25	50	100	25	50	100	25	50	100
2.	94	95	96	95	94	93	95	93	95
3.	95	96	94	93	94	94	94	93	94
4.	95	92	92	92	93	92	91	92	92
Control [a]	95			94			95		

[a] The control seeds were incubated in methanol/water (1:5) for the indicated period.

2.6 References

1. Hambidge M. *J. Nutr.* 2003; **133:** 948S.
2. Lieu PT, Heiskala M, Peterson PA, Yang Y. *Mol. Aspects. Med.* 2001; **22**: 1.
3. Murakami M, Hirano T. *Cancer. Sci.* 2008; **99**: 15.
4. Cole CR, Lifshitz F. *Pediatr. Endocrinol. Rev.* 2008; **5**: 889.
5. Schömann K, Classen HG, Dieter HH, König J, Multhaup G, Rükgauer M, Summer KH, Bernhardt J, Biesalski HK. *Eur. J. Clin. Nutr.* 2002; **56**: 469.
6. Szentmihalyi K, Vinkler P, Fodor J, Balla J, Lakatos B. *Orv. Hetil.* 2006; **147**: 2027.
7. Barceloux DG. *J. Toxicol. Clin. Toxicol.* 1999; **37**: 201.
8. Pandit T. *Ph.D. Thesis*, University of North Bengal, West Bengal, India, 1989.
9. Jorgenson CK. *Inorg. Chim. Acta Rev.* 1968; **2**: 65.
10. Coucouvanis D. *Progr. Inorg. Chem.* 1970; **11**: 233.
11. Bloodworth BC, Demetriov B, Grezeskoviak R. *Inorg. Chim. Acta.* 1981; **53**: L85.
12. Natarajan C, Thariniraj P. *Ind. J. Chem.* 1990; **29A**: 666.
13. Singh H, Srivastava VK, Shukla SN, Upadhyaya MK. *Ind. J. Chem.* 1992; **31A**: 472.
14. Nair MS, Joseyphus RS. *Ind. Chem. Soc.* 2007; **84**: 323.
15. Rosu T, Gulea A, Nicolae A, Georgescu R. *Molecules* 2007; **84**: 782.
16. Cotton FA, Wilkinson G, *Advanced Inorganic Chemistry*, 2nd Ed. Wiley-Inter Science Publishers, New york. 1970.
17. Carlin RL, *Transition Metal Chemistry*, New York and London, 1969, Vol. **5**, pp. 105.
18. Fountain CS, Hatfield WE, *Inorg. Chem.* 1965; **4**: 1366.
19. Kumar N, Suri AK. *Proc. Indian natn. Sci. Acad.* 1980; **46A**: 565.
20. Kumar N, Kalsotra BL, Suri AK. *J. Chinese Chem. Soc.* 1975; **23**: 359.
21. Bickley J, Bonar-Law RP, Borrero Martinez MA, Steiner A. *Inorg. Chim. Acta*, 2004; **357**: 891.
22. Holz RC, Bradshaw JM, Bennett B. *Inorg. Chem.* 1998; **37**: 1219.
23. Akopova OB, Shabyshev LS, Bobrov VL. *Russian Chemical Bulletin*,1995; **44**: 1210.

24. Kozlevčar B, Lah N, Makuc S, Šegedin P, Pohleven F. *Acta Chim. Slov.* 2000; **47**: 421.

25. Waizump k, Takuno M, Fukushima N, Masuda H. *J. Coord. Chem.* 1998; **44**: 269.

26. Bin Z, Jianli L, Wei C, Yunxia W, Zhen S. *Chinese J. Chem.* 2010; **28**: 111.

27. Vučković G, Stanić V, Sovilj Sp, Antonijević-Nikolić M, Mroziński J. *J. Serb. Chem. Soc.* 2005; **70**: 1121.

28. Zevaco TA, Görls H, Dinjus E. *Ingor. Chem Com.* 1998; **1**: 170.

29. Zevaco TA, Görls H, Dinjus E. *Inorg. Chim. Acta.* 1998; **269**: 283.

30. Hamed E, Attia MS, Bassiouny K. *Bioinorg. Chem. Appl.* 2009; **2009**:1.

31. Trukhan VM, Pierpont CG, Jensen KB, Nordlander E, Shteinman AA. *Chem. Commun.* 1999; 1193.

32. Ghattas W, Serhan Z, Bakkali-Taheri NE, Réglier M, Kodera M, Hitomi Y, Simaan AJ. *Inorg. Chem.* 2009; **48**: 3910.

33. Grant CM, Knapp MJ, Huffman JC, Hendrickson DN, Christou G. *Chem. Commun.* 1998; 1753.

34. Moon D, Kim J, Oh M, Suh BJ, Lah MS. *Polyhedron.* 2008; **27**: 447.

35. Maryudi, Yunus RM, Nour AH, Abidin MH. *J. Appl. Sci.* 2009; **9**: 3156.

36. Rardin RL, Poganiuch P, Bino A, Goldberg DP, Tolman WB, Liu S, Lippard JS. *J.* Am. *Chem. Soc.* 1992; **114**: 5240.

37. Randhawa B, Gandotra K, *Thermal Analysis and Calorimetry.* 2006; **85**: 417.

38. Masoud MS, Abou El Enien SA, Kamel HM. *Ind. J. Chem.* 2002; **41A**: 297.

39. Golobič A, Ožbolt L, Pohleven F, Leban I, Šegedin P. *Acta Chim. Slov.* 2006; **53**: 238.

40. Kozlevčar B, Lah N, Leban I, Turel I, Šegedin P, Petrič M, Pohleven F, White AJP, Williams DJ, Giester G. *Croatica Chim. Acta.* 1999; **72** (2–3): 427.

41. Shahzadi S, Ali S, Jabeen S, Kanwal N, Rafique U, Khan AN. *Russian J. Coord. Chem.* 2008; **34**: 38.

42. Chandra S, Sharma AK. *Research Letters in Inorganic Chemistry.* Volume 2009(2009), Article ID 945670, **DOI**:10.1155/2009/945670.

43. Petrič M, Pohleven F, Turel I, Egedin PŠ, White AJP, Williams DJ. Polyhedron. 1998; **17**: 255.

44. Sheldric GM. *Acta Cryst.* 2008; **A64**: 112.

45. Sheldric GM. *SADABS*. University of Göttingen. Germany, 1996.

46. Farrugia LJ. *J. Appl. Cryst.* 1997; **30**: 565.

47. Brandenburg K. *DIAMOND*. Crystal Impact GbR, Bonn, Germany, 2006.

48. Rouxel T, Sarniget A, Kollmann A, Bousquet JF. *Physiol. Mol. Plant Pathol.* 1989; **34**: 507.

49. Kamruddin Sk. Ph.D Thesis, University of North Bengal, West Bengal, India, 1996.

50. Chantrapromma S, Usman A, Fun HK, Poh BL, Karalai C. *J. Mol. Str.* 2004; **688**: 59.

51. Sandhu GK, Boparoy NS. *J. Organomet. Chem.* 1992; **423**: 183.

52. Dutta RL, Saymal A. *Elements of Magnetochemistry*. S. Chand and Company Ltd., 1982.

53. Hasanvand F, Nosrollahi N, Vajed A, Amani S. *Malays. J. Chem.* 2010; **12(1)**: 27.

54. Selwood PW. "Magnetochemistry" 2nd Ed., *Interscience*, New York 1956.

55. Kato M, Jomassen HB, Fanning JC. *Chem. Rev.* 1964; **64(2)**: 99.

56. Patel RN, Pandey HC, Pandeya KB. *Transition Met. Chem.* 1999; **24**: 35.

57. Asefa W, Raju VJT, Chebude Y, Retta N. *Bull. Chem. Soc. Ethiop.* 2009; **23(2)**: 187.

58. Venkatswara Rao B. *J. Therm. Anal. Calorim.* 2010; **100**: 577.

59. Tahir MN, Ülkü D, Mövsümov EM. *Acta Cryst.* 1996; **C52**: 1392.

60. Yang G, Zhu H-G, Zhang L-Z, Cai Z-G, Chen X-M. *J. Chem.* 2000; **53**: 601.

61. Jin Y, Che YX, Zheng JM. *Inorg. Chim. Acta*. 2008; **361**: 2799.

62. Allen FH. *Acta Cryst.* 2002; **B58**: 380.

63. Sugavanam B. *Tin and its Uses*. 1980; **126**: 4.